

^2H NMR in nearly stoichiometric yttrium dideuteride

O.J. Zogal^{1,a}, A.H. Vuorimäki², and E.E. Ylinen²

¹ W. Trzebiatowski Institute for Low Temperature and Structure Research, Polish Academy of Sciences, ul. Okólna 2, 50-950 Wrocław, Poland

² Wihuri Physical Laboratory, Department of Physics, University of Turku, 20014 Turku, Finland

Received 8 September 1998

Abstract. ^2H NMR spectra and spin-lattice relaxation rates, R_1 are measured as functions of temperature (4.2–310 K) for $\text{YD}_{1.99}$ and $\text{YD}_{1.99+0.04}$. In $\text{YD}_{1.99}$ the measured temperature dependence of R_1 is explained by the interaction of deutron spins with conduction electrons and the value $7.56 \times 10^{-5} \text{ s}^{-1} \text{ K}^{-1}$ is obtained for the inverse Korringa product R_{1e}/T . Most of the spectral features in the “rigid” lattice regime are described by the dipolar interaction. No evidence of the deuterium self-diffusion was observed in the measured temperature range. The low-temperature spectra in $\text{YD}_{1.99+0.04}$ consisted of two components: a central line and a doublet characteristic for the quadrupole interaction. The central line corresponds to zero electric field gradients (EFG) at the sites of the deuterons which have a surrounding with cubic symmetry like in $\text{YD}_{1.99}$. The doublet indicates a non-zero EFG which can be explained in terms of the presence of short-range ordered domains of the hypothetical $\text{YD}_{2.25}$ stoichiometry. Other possible interpretations of the spectra are also discussed. In the vicinity of 250 K both spectra and R_1 reflect the onset of the rapid motion of deuterium atoms. The linear dependence of R_1 at low temperatures yields $R_{1e}/T = 6.35 \times 10^{-5} \text{ s}^{-1} \text{ K}^{-1}$.

PACS. 61.66.Fn Inorganic compounds – 61.18.Fs Magnetic resonance techniques; Mössbauer spectroscopy – 76.60.-k Nuclear magnetic resonance and relaxation

1 Introduction

Nonstoichiometry, which is the characteristic feature of many transition and rare-earth metal hydrides- leads to interesting temperature- and concentration-dependent electronic and structural properties. In particular, an unusual metal-semiconductor (M-S) transition in slightly superstoichiometric yttrium dihydride, $\text{YH}_{2.10}$ was reported by Vajda and Daou [1]. They observed a semiconducting phase with a very narrow gap below 60–80 K besides the usual transition at 235–260 K. The usual transition was described in terms of an order-disorder transformation of the octahedral hydrogen sublattice. Further studies by the same authors [2] showed that the order-disorder transformation above 200 K is not very stable and the M-S transition depends on the direction of the temperature run. Moreover, the latter depends very critically on stoichiometry (*i.e.* x in YH_{2+x}) and ordering is not necessarily lead to a M-S transition. X-ray diffraction data [2] indicate ordering of the H octahedral sublattice below room temperature already when x is above 0.05 while the M-S transition is observed for $x = 0.095$ under a quench condition. A structural ordering was observed in terbium [3] and lanthanum [4] deuterides, where the nominal FCC metal lattice structure exists over a wider range of deuterium concentration than in yttrium hydrides. Neutron diffraction

studies in TbD_{2+x} [3] and $\text{LaD}_{2.25}$ [4] revealed that octahedral site hydrogens undergo long-range ordering at lower temperatures (below room temperature). In the former, the ideal composition corresponds to a Ni_3Mo type structure (I4/mmm). This structure is stoichiometric at 25% octahedral deuterium. For nonstoichiometric $\text{TbD}_{2.18}$ [3] a good agreement between calculated and observed line intensities was obtained if about 20% of the x -deuterium atoms are randomly distributed on vacant octahedral sites of the perfectly ordered Ni_3Mo type of structure. Analysis of the neutron diffraction data for $\text{LaD}_{2.25}$ [4] confirmed the structure, earlier proposed for $\text{TbD}_{2.18}$, although some displacements from the ideal tetrahedral deuterium and La positions are very probable. Also a very small partial occupation of the other octahedral sites (O(2)) gave a slightly better agreement between the calculated and observed parameters. Another technique, neutron vibration spectroscopy, was used to investigate the structural properties of the hydrides TbH_{2+x} [5], LaH_{2+x} [6,7] and YH_{2+x} [7]. In all these systems, the structural ordering within the octahedral hydrogen sublattice was observed. In $\text{YH}_{2.03}$ the octahedral hydrogen atoms are predominantly isolated in a local cubic environment, but a small fraction of these atoms form small clusters of short-range order. As the hydrogen concentration increases, the short-range order increases, too.

^a e-mail: zogal@highscreen.int.pan.wroc.pl

In this paper we present ^2H NMR results of two samples: $\text{YD}_{1.99}$ and $\text{YD}_{1.99+0.04}$, as representatives for cases with no and with some octahedral sites occupied, respectively. The ordering of the octahedral H sublattice and the transition to the disordered state are expected to be observed by temperature variation.

2 Experimental

The samples were prepared from 99.99 at% pure yttrium metal obtained from the Ames Laboratory (Ames, Iowa). Synthesis of the yttrium deuterides followed a two-step procedure, similar to that established by Vajda *et al.* [8]. In the first step, about 1 g of Y metal was loaded at 600-650 °C with D_2 by gas-phase absorption in a quartz tube to the nominal D/Y stoichiometry of 2. After thermal equilibration the sample was evacuated to remove any excess of octahedrally coordinated deuterium, which is known to be unstable at these temperatures. In this way, a “pure” dideuteride, $\text{YD}_{1.99}$ was obtained. The $\text{YD}_{2.03}$ ($\text{YD}_{1.99+0.04}$) sample was made by adding the additional deuterium atoms, at 250-300 °C to an $\text{YD}_{1.99}$ sample. The concentrations were determined by pressure-difference measurements with a Baratron manometer to the accuracy of ± 0.012 for the ratio D/Y.

The NMR measurements were performed with a Bruker MSL-300 pulse spectrometer at the frequency of 30.73 MHz using a Thor superconducting magnet. The probe and the cryostat were home-made. The saturation-recovery sequence with a series of 3-5 saturation pulses of 13-17 μs separated by 0.5-0.9 ms was used to measure the spin-lattice relaxation time T_1 . At least one value of the waiting time τ was long enough to allow the magnetisation $M(\tau)$ to reach essentially its equilibrium value $M(\infty)$. T_1 was obtained by fitting $M(\tau)$ to a simple exponential function $M(\tau) = C_1[1 - C_2 \exp(-\tau/T_1)]$ where C_1 , C_2 and T_1 were parameters. The parameter C_1 was essentially $M(\infty)$ and C_2 was very close to 1.0 indicating a nearly full saturation. The ^2H NMR spectra were obtained by making the Fourier transform of the ^2H free induction decay following a single pulse of 1 μs . This pulse was sufficiently short to uniformly irradiate the broadest deuterium NMR spectrum (ca. 16 kHz for $\text{YD}_{1.99+0.04}$), that was observed at temperatures where the deuterium diffusion was frozen out.

3 Results and discussion

3.1 Analysis of $\text{YD}_{1.99}$ data

The deuterium spin-lattice relaxation rate $R_1 = 1/T_1$ is shown in Figure 1 for $\text{YD}_{1.99}$. The temperature dependence can be well described as

$$R_1 = A + BT \quad (1)$$

where $A = (8.9 \pm 1.3) \times 10^{-4} \text{ s}^{-1}$, $B = (7.56 \pm 0.08) \times 10^{-5} \text{ K}^{-1} \text{ s}^{-1}$ and T is the temperature. Such

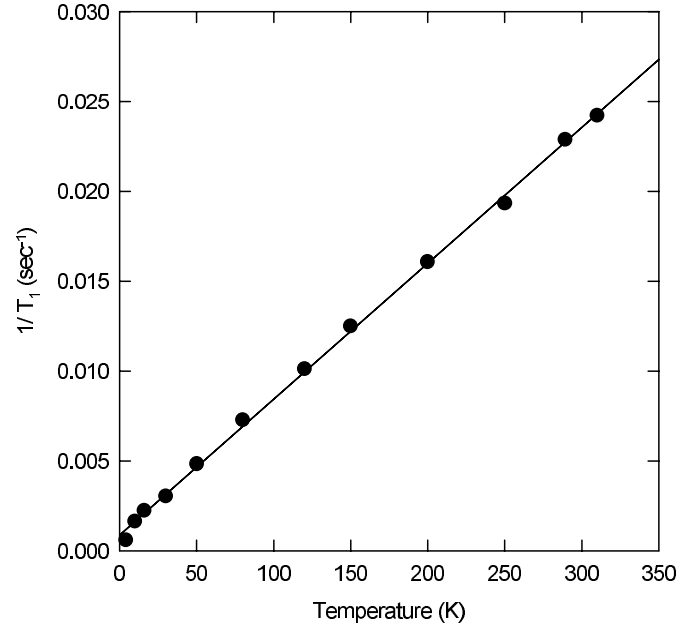


Fig. 1. Temperature dependence of the measured deuterium spin-lattice relaxation rate, $1/T_1$ in $\text{YD}_{1.99}$. The open circles are experimental points and the solid line represents the fit to equation (1).

behaviour is expected when the diffusion of deuterium is negligible and then the parameter A is the relaxation rate (R_{1p}) due to the presence of paramagnetic ions in the metal lattice whereas B corresponds to the usual Korringa relaxation (R_{1e}) *via* conduction electrons. The effects of paramagnetic impurities on the measured relaxation rates in hydrides have been discussed in a number of papers [9–12]. Torgeson *et al.* [11] came to the conclusion that for sufficiently low impurity concentration R_{1p} can be regarded essentially as temperature independent. They also suggested that the value of R_{1e} is the true one 1) if the 77 K point lies on the straight line fitted to the data and 2) if the interception is less than 0.2 s^{-1} . Both criteria are fulfilled in our case, although, since we observe deuterium resonance, the second requirement is more stringent now *i.e.* $0.2(\frac{2D}{\gamma_P})^2 = 4.7 \times 10^{-3} \text{ (s}^{-1}\text{)}$ (slow spin-diffusion limit for the paramagnetic ions) and $0.2(\frac{2D}{\gamma_P})^{2.75} = 1.2 \times 10^{-3} \text{ (s}^{-1}\text{)}$ (fast spin-diffusion case). Thus, the parameter B characterises reliably the strength of the hyperfine interactions in the studied deuteride.

A similar value of B , equal to $7.1 \times 10^{-5} \text{ K}^{-1} \text{ s}^{-1}$ was estimated for $\text{YD}_{1.98}$ by Markert [13] from T_1 measurements at temperatures above 294 K, where the diffusion of deuterium already, to some extent, contributes to the spin-lattice relaxation. As noted by Nowak, Zogal and Minier [14], in titanium-niobium hydrides, to a good approximation, R_{1e} can be expressed as

$$R_{1e} = R_{1s} + R_{1d} \quad (2)$$

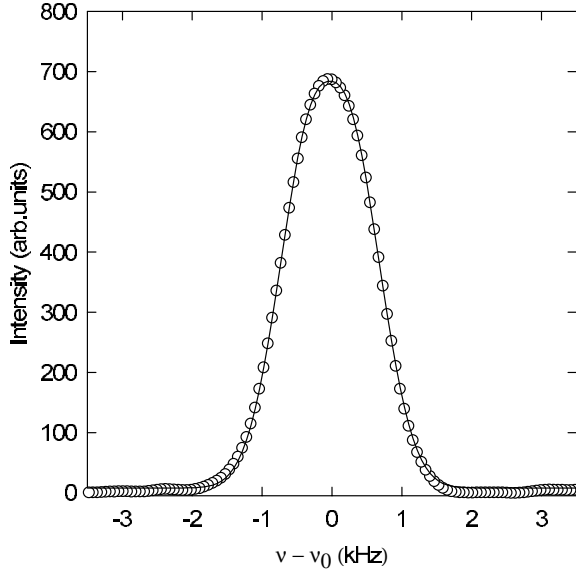


Fig. 2. Deuteron absorption line (open circles) at 10 K and at the resonance frequency of 30 MHz in $\text{YD}_{1.99}$. The full line represents the fit to equation (3) with $C = 676$, $b = 1.38$ and $n = 2.44$.

where

$$R_{1s} = 4\pi\hbar\gamma_{\text{H}}^2 k_{\text{B}} [H_{\text{hfs}}(s)N_{\text{s}}(E_{\text{F}})]^2 T$$

$$R_{1d} = 4\pi\hbar\gamma_{\text{H}}^2 k_{\text{B}} [H_{\text{hfs}}(d)N_{\text{d}}(E_{\text{F}})]^2 qT.$$

$H_{\text{hfs}}(s)$ in equation (2) is the hyperfine field at the proton due to the Fermi-contact interaction with unpaired s electrons at E_{F} , $H_{\text{hfs}}(d)$ is the hyperfine field resulting from the core polarisation of spin-paired s orbitals at energies below E_{F} by unpaired d electrons at E_{F} , $N_{\text{s}}(E_{\text{F}})$ and $N_{\text{d}}(E_{\text{F}})$ are the s - and d -band electron densities of states at Fermi level, q is a numerical reduction factor arising from the d -band degeneracy, γ_{H} is the gyromagnetic ratio for protons and the other parameters have their common meanings. As it follows from equation (2), R_{1e} is proportional to the square of the nuclear gyromagnetic ratio and therefore $R_{1e}(^1\text{H}) = (\frac{\gamma_{\text{H}}}{\gamma_{\text{D}}})^2 R_{1e}(^2\text{H})$. Assuming that hydrides and deuterides are identical for a given concentration, we estimate $R_{1e}(^1\text{H})/T = 3.21 \times 10^{-3} \text{ s}^{-1} \text{ K}^{-1}$ for $\text{YH}_{1.99}$. In fact, Torgeson *et al.* [11] reported $R_{1e}(^1\text{H})/T = 2.86 \times 10^{-3} \text{ s}^{-1} \text{ K}^{-1}$ for $\text{YH}_{1.98}$, which has the composition very close to $\text{YH}_{1.99}$. A small difference between these two $R_{1e}(^1\text{H})/T$ values could be attributed to isotope effects and to the quadrupolar interaction. The deuteron quadrupole moment interacts with the total electric field gradient due to all the surrounding charges [15]. Therefore the quadrupole relaxation is even more sensitive than the dipolar relaxation to any local field fluctuations at the quadrupole nucleus [16].

A typical ^2H NMR line shape observed at $T = 10 \text{ K}$ is shown in Figure 2. The lineshape can be very well fitted to a modified Gaussian function [17]:

$$f(\nu) = C \exp(-b|\nu - \nu_0|^n) \quad (3)$$

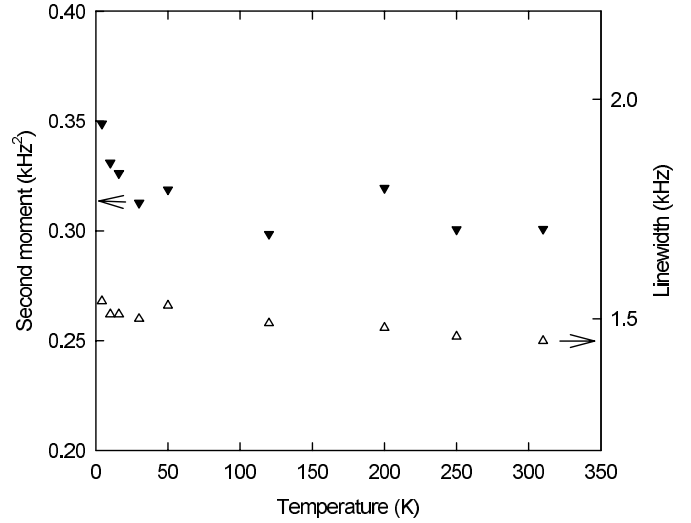


Fig. 3. Temperature dependence of the linewidth (the triangles up) and the second moments (the filled triangles down) in $\text{YD}_{1.99}$. The data result from the best fits of equation (3) to the experimental resonance lines.

where C , b and n are fitting parameters. As these parameters are found by the least squares method, the linewidth and the moments can be determined. In particular, the linewidth $\Delta\nu_{1/2}$ and the second moment M_2 are given by

$$\Delta\nu_{1/2} = 2 \left(\frac{\ln 2}{b} \right)^{1/n}$$

$$M_2 = \left(\frac{1}{b} \right)^{2/n} \frac{\Gamma(\frac{3}{n})}{\Gamma(\frac{1}{n})}$$

where $\Gamma(z)$ is the gamma function of z . The values for $\Delta\nu_{1/2}$ and M_2 obtained in this way are shown in Figure 3 as functions of temperature. They are almost temperature independent in the measured temperature range which indicates that deuteron diffusion is frozen out and we may assume that the main contribution responsible for the observed line shape comes from the nuclear dipole-dipole coupling in so called “rigid” lattice regime. Therefore, the second moment of the deuteron resonance can be calculated from Van Vleck [18] formula for a powder

$$M_2 = \frac{3}{5} \left(\frac{1}{2\pi} \right)^2 \gamma_I^4 \hbar^2 I(I+1) \sum_i r_{ij}^{-6}$$

$$+ \frac{4}{15} \left(\frac{1}{2\pi} \right)^2 \gamma_S^2 \gamma_I^2 \hbar^2 S(S+1) \sum_k r_{kj}^{-6} \quad (4)$$

where, I and S are the nuclear spins of deuterium and yttrium, γ_I and γ_S are the corresponding gyromagnetic ratios, r_{ij} and r_{kj} are the distances from deuteron j to deuteron i and to yttrium k , respectively. If we use the lattice parameter $a_0 = 0.5197 \text{ nm}$ (at room temperature) for the fcc structure of $\text{YD}_{1.99}$ and the appropriate lattice sums for the CaF_2 structure [19], we can calculate $M_2 = 0.266 \text{ kHz}^2$ from equation (4). The major contribution to it comes from the $^2\text{H}-^2\text{H}$ dipole-dipole interaction

(ca. 98%) whereas the ^2H - ^{89}Y interaction is of much less importance. In addition to the second moment, the fourth moment or equivalently the ratio $M_4/(M_2)^2$ characterises the observed resonance lineshape. M_2 and M_4 describe the lineshape more accurately than M_2 alone and limit the number of possible crystal structures to those which have the same values of M_2 and $M_4/(M_2)^2$.

Using the calculation method of Nowak *et al.* [20], the ratio $M_4/(M_2)^2 = 2.62$ was obtained for $\text{YD}_{1.99}$ when the ^2H - ^{89}Y contribution to M_2 and M_4 was neglected. The experimental values $M_2 = 0.30 \text{ kHz}^2$ and $M_4/(M_2)^2 = 2.65$ at 250 K are in a reasonable agreement with the calculated ones. Thus, the dipole-dipole interaction mainly determines the observed lineshape. The small deviation between the theoretical values and the observed ones could be due to the experimental accuracy and quadrupole effects. The latter might originate from the local imperfections caused by vacancies, strains, dislocations etc. In this case, the quadrupole contribution to the second moment for a powder is given by [21],

$$\langle \Delta\nu^2 \rangle_q = \frac{9}{400} \left(\frac{e^2 q Q}{h} \right)^2 \frac{(2I+3)}{I^2(2I-1)} \quad (5)$$

where e is the electronic charge, Q is the quadrupole moment of the deuteron nucleus and eq is the electric field gradient at the deuterium site, created by the non-cubic environment. If the whole difference between the experimental and calculated second moments is assumed to result from the quadrupole coupling, the value 0.55 kHz for the quadrupole coupling constant ($\frac{e^2 q Q}{h}$) can be calculated from equation (5). Since there are also other contributions to the mentioned difference, the real quadrupole coupling constant (QCC) could be even smaller.

3.2 Analysis of $\text{YD}_{1.99+0.04}$ data

The observed resonance line of deuterons in $\text{YD}_{1.99+0.04}$ typical for low temperatures (4.2 – 250 K) is shown in Figure 4. It contains two components: a symmetrical central line with the shape found in $\text{YD}_{1.99}$ and a doublet, typical for the quadrupole interaction. The former shape can be described by using equation (3) as in the case of $\text{YD}_{1.99}$. The second resonance line seems to have a shape with quadrupolar origin, typical for deuterons with spin $I = 1$. The fraction of the first component, estimated from the area is ca. 0.8 of the total intensity. The QCC evaluated from the doublet separation of the second component is 9.6 kHz. This value is somewhat underestimated because the additional dipolar broadening tends to make the separation of the maxima in the doublet smaller. The main difference between $\text{YD}_{1.99}$ and $\text{YD}_{1.99+0.04}$ is the excess of deuterium in the latter where deuterons start to occupy the octahedral sites.

The tetrahedral (T) and octahedral (O) sites have sufficiently high symmetry to cancel the electric field gradient (EFG) at both sites. Nevertheless, the T sites with one or more nearest neighbours in O sites have a distorted environment and thus a nonzero EFG and static quadrupole

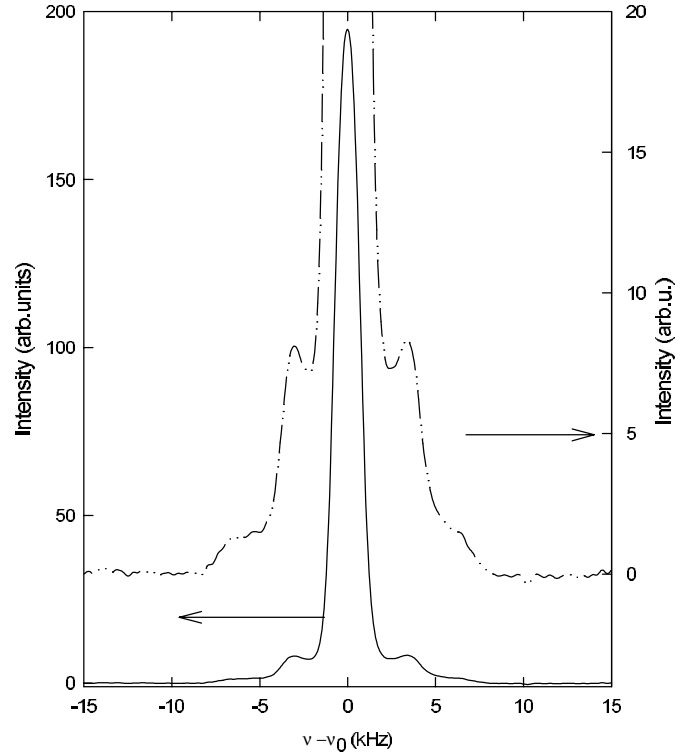


Fig. 4. NMR spectrum of ^2H in $\text{YD}_{1.99+0.04}$ at $T = 7 \text{ K}$. It represents a superimposition of the 1.45 kHz wide (FWHM) central component and the component with the quadrupole splitting ($\frac{3}{4} \frac{e^2 q Q}{h} = 7.2 \text{ kHz}$). The upper line shows the spectrum in an enlarged scale.

interaction. Assuming a random occupation of the O sites, we can estimate that the probability of a T site with no nearest neighbours in O sites is $(1 - 0.04)^4 = 0.849$, because each T site has four nearest octahedral sites and each O site is vacant with the probability $(1 - 0.04)$. The calculated fractional concentration (0.849) is somewhat larger than the empirical one (0.8). That difference could be explained by assuming that the deuteron concentration of $\text{YD}_{1.99+0.04}$ is actually slightly higher, *i.e.* $\text{YD}_{1.99+0.054}$. Earlier, the random occupation of the O sites was proposed by Adolphi *et al.* [22] to interpret the ^2H NMR spectra of $\text{YD}_{1.98}$ and $\text{YD}_{2.08}$ at 195 K. They obtained the difference spectrum by subtracting the $\text{YD}_{1.98}$ spectrum from the $\text{YD}_{2.08}$ spectrum and modelled that difference spectrum by assuming that it corresponds to the structurally distorted T sites and the distortion is caused by randomly occupied O sites. However, the difference spectrum did not display the resolved quadrupolar features as we observed (Fig. 4) and the value of QCC was not given. The exact reason for the different spectra of our $\text{YD}_{1.99+0.04}$ and their $\text{YD}_{2.08}$ is not clear, but some possibilities can be mentioned. The D/Y ratio in $\text{YD}_{2.08}$ is probably smaller than 2.08, because a value 2.066 ± 0.01 was estimated from the MAS NMR experiment [22]. On the other hand, the properties of yttrium hydrides in the range from $\text{YH}_{2.00}$ to $\text{YH}_{2.10}$ are very sensitive to the H/Y ratio [2]. There is also some unknown amount of deuterium

“located” in a sharp rip in the difference spectrum [22], which remains to be explained. In addition, the $\text{YD}_{2.08}$ spectrum was observed at 195 K, close to the temperature of 200 K, where we observed the quadrupole splitting, but with rather low signal to noise ratio. Therefore, experiments at a much lower temperature than 195 K could help to understand the difference between the present ^2H NMR spectra and those of Adolphi *et al.* [22].

Another possible interpretation for the $\text{YD}_{1.99+0.04}$ lineshape can also be found. The short-range and long-range ordering in the O hydrogen sublattice was suggested by the observation of resistivity anomalies [1, 2]. This phenomenon was confirmed by neutron diffraction [3, 4] and neutron vibrational spectroscopy [7]. In YH_{2+x} , where $x \cong 0.05$ and 0.03, the domains with a short range structural ordering within the O hydrogen sublattice were indicated [2, 7]. The short-range arrangement was connected to the long-range (I4/mmm) order expected for the hypothetical cubic $\text{YH}_{2.25}$ stoichiometry. Each hydrogen in a T site of that structure has one nearest neighbour in an O site and the axially symmetric EFG tensor may have a non-zero value at the T site. The O site, in turn has a cubic environment and a zero EFG tensor is expected. The fraction of the T sites is 8/9 and the fraction of the O sites is 1/9 of the total hydrogen concentration. Let us assume that in $\text{YD}_{1.99+0.04}$ we have, besides $\text{YD}_{1.99}$ (the actual “pure” dihydride composition), small domains of short-range ordered $\text{YD}_{2.25}$. Then, for 80% concentration of the former and 20% of the latter, we obtain $0.8 \times 1.99 + 0.2 \times 2.25 = 1.642$ for the number of undistorted sites and $0.2 \times 2.00 = 0.4$ for distorted sites giving the total composition of $1.642 + 0.4 = 2.042$. It corresponds to the fraction of $0.4/2.042 = 0.196$ for the quadrupole splitted resonance line and 0.804 for the non-splitted line. Since both interpretations for the observed ^2H NMR spectrum in $\text{YD}_{1.99+0.04}$ seem to be reasonable, a “mixed” situation can also be considered, *i.e.* one part of the O sites is occupied randomly and another part of them forms ordered domains ($\text{YD}_{2.25}$). This interpretation was applied to the neutron scattering data of $\text{YH}_{2.03}$ and $\text{LaH}_{2.03}$ [6, 7]. For $\text{LaH}_{2.03}$ it was estimated that 37% of the hydrogen atoms in the O sites were in short-range-ordered domains.

Observation of the resolved features in our sample indicates that either it contains the ordered structure of $\text{YD}_{2.25}$ together with $\text{YD}_{1.99}$ or ordered domains within the disordered structure of randomly occupied O sites. Additional studies, by neutron scattering for example, should be made to check which interpretation is correct.

In ^2H NMR studies of lanthanum deuterides [23] the $\text{LaD}_{2.28}$ sample (the lowest concentration of deuterium in those deuterides) gave a spectrum with three lines. One with no quadrupolar splitting, one with an axially symmetric EFG tensor and one with a highly asymmetric EFG tensor. The QCC for the second line was estimated to be 9.5 kHz, which is close to the value found for the $\text{YD}_{1.99+0.04}$ sample.

The line shape (Fig. 4) remains nearly constant from 4.2 K to about 200 K. However, in the vicinity of 250 K

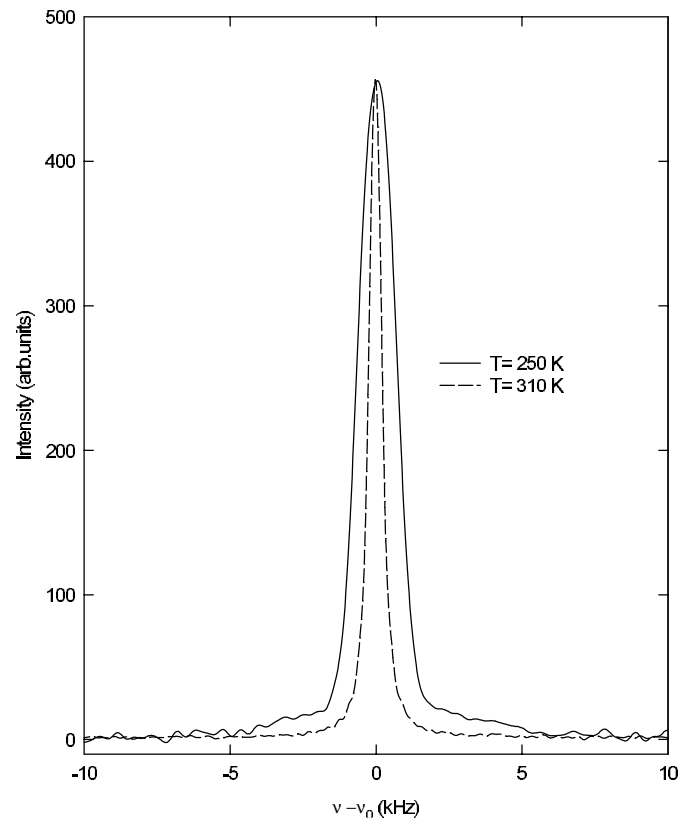


Fig. 5. ^2H NMR spectra in the high temperature range in $\text{YD}_{1.99+0.04}$. The quadrupole features are still observable at 250 K but not at 310 K where the Lorentzian function describes the whole spectrum as typical for motional narrowing.

some changes are observed. The quadrupole features vanish and the line width of the central component starts to decrease. The experimental spectra at 250 K and 310 K are shown in Figure 5. At 310 K (the highest temperature in our experiments) a single symmetric Lorentzian line is observed. The temperature dependence of the linewidth of the central component together with the spin-lattice relaxation rates is shown in Figure 6. The line narrowing and the deviation of R_1 from the linear dependence at the high-temperature range reflect a rapid deuterium motion. The diffusive motion causes a fluctuation of dipolar and quadrupolar interactions. As the result, the spin-lattice relaxation rate of equation (1) has an additional term [24, 25]

$$R_1 = C_m \left(\frac{\tau_d}{1 + (2\pi\nu_0\tau_d)^2} + \frac{4\tau_d}{1 + 4(2\pi\nu_0\tau_d)^2} \right) + C_q \left(\frac{\tau_q}{1 + (2\pi\nu_0\tau_q)^2} + \frac{4\tau_q}{1 + 4(2\pi\nu_0\tau_q)^2} \right) \quad (6)$$

where C_m and C_q are constants and τ_d and τ_q are the correlation times of the deuterium motion characteristic for dipolar and quadrupolar interactions, respectively. Often $\tau_{d,q}$ obeys the Arrhenius relation

$$\tau_{d,q} = \tau_{d,q}(0) \exp(E_{d,q}/kT)$$

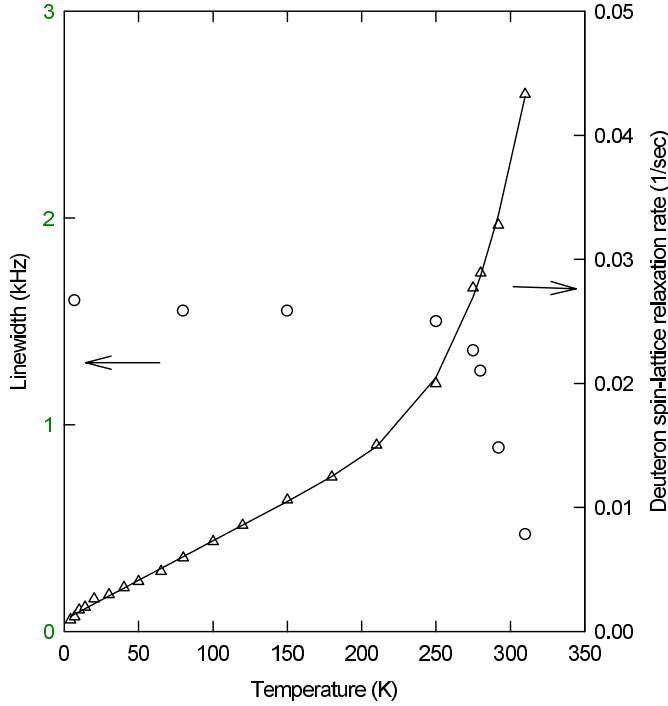


Fig. 6. Temperature dependence of the linewidth of the central component (the scale on the left) and the spin-lattice relaxation rate (the scale on the right) in $YD_{1.99+0.04}$. Note the onset of the line narrowing and the deviation of R_1 from the linear dependence near 250 K.

where $E_{d,q}$ is the activation energy for dipolar (d) and quadrupolar (q) interactions, respectively, and k is the Boltzmann constant. In the temperature region, where $\nu_0\tau_{d,q} \gg 1$, and one of the two interactions dominates, equation (6) gives $R_{1d,q} = C \exp(-E_a/kT)$. Here E_a is the activation energy for the dominating mechanism and $C = 2C_{m,q}/[(2\pi\nu_0)^2\tau_{d,q}(0)]$. Then, the total relaxation rate is

$$R_1 = A + BT + C \exp(-E_a/kT). \quad (7)$$

The R_1 data of Figure 6 can be fitted to equation (7) with the following parameters:

$$\begin{aligned} A &= (10 \pm 1.5) \times 10^{-4} \text{ s}^{-1}, \\ B &= (6.35 \pm 0.15) \times 10^{-5} \text{ s}^{-1} \text{ K}^{-1}, \\ C &= 45 \pm 13 \text{ s}^{-1}, \\ E_a/k &= 2360 \pm 90 \text{ K} \quad (0.20 \pm 0.01 \text{ eV}). \end{aligned}$$

The value of A is close to that for $YD_{1.99}$ as can be expected because of the similar impurity content. The parameter B is somewhat smaller than for $YD_{1.99}$, indicating a lower density of electronic states at the Fermi level. It follows from equation (2) that

$$R_{1e} \propto N^2(E_F) \left[r \frac{N_s^2(E_F)}{N^2(E_F)} + s \frac{N_d^2(E_F)}{N^2(E_F)} \right]$$

where $N(E_F) = N_s(E_F) + N_d(E_F)$ and, if we assume that the term in square brackets does not vary much with deu-

terium concentration,

$$\frac{N(E_F)\{YD_{1.99+0.04}\}}{N(E_F)\{YD_{1.99}\}} \propto \sqrt{\frac{R_{1e}(YD_{1.99+0.04})}{R_{1e}(YD_{1.99})}} = 0.92.$$

This shows diminishing of $N(E_F)$ due to the withdrawal of electrons from the Fermi level to form a bonding with deuterium atoms in octahedral sites. Similarly, in the La-H system R_{1e} of protons was observed to decrease with increasing hydrogen content [26].

The activation energy $E_a = 0.20$ eV found here is much smaller than $E_a = 0.55$ eV reported for $YD_{2.04}$ and $YD_{2.08}$ on the basis of ^2H NMR with selective inversion/magnetisation transfer experiments [22]. A small E_a has been reported earlier, 0.34 eV for $YH_{1.98}$ [27], but it is still higher than our value. Hence, additional measurements of R_1 are needed over a larger temperature range than in our research. In particular, the temperature interval should include the area where the maximum of R_1 is expected. On the other hand, a low E_a (0.2 eV) was determined for the proton self-diffusion in lanthanum hydride $LaH_{2.90}$ [28] in the temperature range where the coexistence of the ordered and disordered phases is very probable.

4 Conclusions

It has been shown that small differences in the stoichiometry of yttrium deuteride near YD_2 composition have a remarkable influence on the structural and electronic properties of the deuteride. For the almost stoichiometric dideuteride ($YD_{1.99}$), the ^2H NMR spectrum consists of a single line with the shape well described in terms of the dipolar interaction between the nuclei. The spin-lattice relaxation rate exhibits the linear dependence, characteristic for the Korringa relaxation *via* conduction electrons. A small excess of deuterium in YD_2 ($YD_{1.99+0.04}$ in our case) causes changes in the spectrum and spin-lattice relaxation rate. In the low-temperature range the spectrum consists of two components: a central line similar to that previously observed in $YD_{1.99}$ and a doublet due to the quadrupolar interaction. The central line originates from the deuterium atoms located in the sites of cubic symmetry, while the doublet is due to an axially symmetric field gradient. In general, a non-zero EFG at tetrahedral sites is produced by the deuterium atoms located in the octahedral sites. The earlier ^2H NMR studies in the same system [22] showed a component with quadrupolar influence but without any structure. It was interpreted in terms of a random occupation of octahedral sites. We do not completely exclude such a possibility but propose another one. That is the presence of ordered domains which would have the $YH_{2.25}$ composition with $I4/mmm$ superstructure, found in analogous compounds TbD_{2+x} [3] and $LaD_{2.25}$ [4]. The observed quadrupolar features would be due to these ordered domains. The disordered phase would be responsible for the central component of the low-temperature spectrum. At temperatures near 250 K and

above, the spectra and the spin-lattice relaxation rates indicate the beginning of thermally activated rapid motion of the deuterium atoms. The fit to the temperature dependence of R_1 in $\text{YD}_{1.99+0.04}$ yields a smaller value for the inverse Korringa product ($R_{1e}T^{-1}$) than in $\text{YD}_{1.99}$. This is consistent with earlier studies in lanthanum hydrides [26], implying the decrease of the electron density of states at Fermi level with the increase of hydrogen concentration. The activation energy estimated from the fit is smaller than previously reported [22] for the same system, but the same as reported for lanthanum hydride, $\text{LaH}_{2.90}$ in the temperature range where ordered and disordered phases coexist [28]. Measurements of the spin-lattice relaxation at higher temperatures in the $\text{YD}_{1.99+0.04}$ sample are suggested in order to check the low activation energy obtained in this research.

This work has been financially supported by the KBN (Project N0.2P03B 07411), by the exchange program between Polish and Finnish Academies and by the University of Turku.

References

1. P. Vajda, J.N. Daou, *Phys. Rev. Lett.* **66**, 3176 (1991).
2. J.N. Daou, P. Vajda, *Phys. Rev. B* **45**, 10907 (1992).
3. G. Andre, O. Blaschko, W. Schwarz, J.N. Daou, P. Vajda, *Phys. Rev. B* **46**, 8644 (1992).
4. T.J. Udovic, Q. Huang, J.J. Rush, J. Schefer, I.S. Anderson, *Phys. Rev. B* **51**, 12116 (1995).
5. T.J. Udovic, J.J. Rush, I.S. Anderson, *Phys. Rev. B* **50**, 7144 (1994).
6. T.J. Udovic, J.J. Rush, I.S. Anderson, *J. Phys.-Cond. Matter* **7**, 7005 (1995).
7. T.J. Udovic, J.J. Rush, Q. Huang, I.S. Anderson, *J. Alloys Comp.* **253-254**, 241 (1997).
8. P. Vajda, J.N. Daou, J.P. Burger, *Phys. Rev. B* **36**, 8669 (1987).
9. T.-T. Phua, B.J. Beaudry, D.T. Peterson, D.R. Torgeson, R.G. Barnes, M. Belhoul, G.A. Styles, E.F.W. Seymour, *Phys. Rev. B* **28**, 6227 (1983).
10. T.-T. Phua, D.R. Torgeson, R.G. Barnes, R.J. Schoenberger, B.J. Beaudry, D.T. Peterson, M. Belhoul, G.A. Styles, E.F.W. Seymour, *J. Less-Common Met.* **104**, 105 (1984).
11. D.R. Torgeson, L.-T. Lu, T.-T. Phua, R.G. Barnes, D.T. Peterson, E.F.W. Seymour, *J. Less-Common Met.* **104**, 79 (1984).
12. J.-W. Han, D.R. Torgeson, R.G. Barnes, *Phys. Rev. B* **42**, 7710 (1990).
13. J.T. Markert, Ph.D. thesis, Cornell University (1987).
14. B. Nowak, O.J. Zogal, M. Minier, *J. Phys. C* **12**, 4591 (1979).
15. R.G. Barnes, in *Topics in Applied Physics*, edited by H. Wipf (Springer Verlag, Berlin, 1997), Vol. 73.
16. H.T. Weaver, *J. Magn. Reson.* **15**, 84 (1974).
17. W.C. Harper, R.G. Barnes, *J. Magn. Reson.* **21**, 507 (1976).
18. J. Van Vleck, *Phys. Rev.* **74**, 1168 (1948).
19. H.S. Gutowsky, B.R. McGarvey, *J. Chem. Phys.* **20**, 1472 (1952).
20. B. Nowak, J. Kowalewski, O.J. Zogal, *J. Magn. Reson.* **54**, 9 (1983).
21. R. Bersohn, *J. Chem. Phys.* **10**, 1505 (1952).
22. N.L. Adolphi, J.J. Balbach, M.S. Conradi, J.T. Markert, R.M. Cotts, P. Vajda, *Phys. Rev. B* **53**, 15054 (1996).
23. D.G. deGroot, R.G. Barnes, B.J. Beaudry, R.G. Torgeson, *J. Less-Common Met.* **73**, 233 (1980).
24. N. Bloembergen, E.M. Purcell, R.V. Pound, *Phys. Rev.* **73**, 679 (1948).
25. A. Abragam, *The Principles of Nuclear Magnetism* (Clarendon Press, Oxford, 1961), p. 314.
26. R.G. Barnes, C.-T. Chang, M. Belhoul, D.R. Torgeson, R.J. Schoenberger, B.J. Beaudry, E.F.W. Seymour, *J. Less-Common Met.* **172-174**, 411 (1991).
27. R.J. Barnfather, E.F.W. Seymour, G.A. Styles, A.J. Dianoux, R.G. Barnes, D.R. Torgeson, *Phys. Chem.* **164**, 935 (1989).
28. R.G. Barnes, B.J. Beaudry, D.R. Torgeson, C.-T. Chang, R.B. Creel, *J. Alloys Comp.* **253-254**, 445 (1997).